Flexible microwave absorbers based on barium hexaferrite, carbon black, and nitrile rubber for 2–12GHz applications

S. Vinayasree, M. A. Soloman, Vijutha Sunny, P. Mohanan, Philip Kurian, P. A. Joy, and M. R. Anantharaman

Citation: Journal of Applied Physics **116**, 024902 (2014); doi: 10.1063/1.4886382
View online: http://dx.doi.org/10.1063/1.4886382
View Table of Contents: http://scitation.aip.org/content/aip/journal/jap/116/2?ver=pdfcov
Published by the AIP Publishing

Flexible microwave absorbers based on barium hexaferrite, carbon black, and nitrile rubber for 2–12 GHz applications

S. Vinayasree,[1,2] M. A. Soloman,[3] Vijutha Sunny,[4] P. Mohanan,[5] Philip Kurian,[6] P. A. Joy,[7] and M. R. Anantharaman[1,a)]

[1]*Department of Physics, Cochin University of Science and Technology, Cochin 682 022, Kerala, India*
[2]*On deputation from Department of Physics, Govt. Victoria College, Palakkad 678 001, Kerala, India*
[3]*Department of Chemistry, St. Albert's College, Cochin 682 018, Kerala, India*
[4]*Departments of Physics, Alphonsa College, Arunapuram P.O, Pala, Kottayam 686 574, Kerala, India*
[5]*Department of Electronics, Cochin University of Science and Technology, Cochin 682 022, Kerala, India*
[6]*Department of Polymer Science and Rubber Technology, Cochin University of Science and Technology, Cochin 682 022, Kerala, India*
[7]*Physical and Materials Chemistry Division, National Chemical Laboratory, Dr. Homi Bhabha Road, Pune 411008, India*

(Received 21 May 2014; accepted 20 June 2014; published online 9 July 2014)

Flexile single layer electromagnetic wave absorbers were designed by incorporating appropriate amounts of carbon black in a nitrile butadiene rubber matrix along with an optimized amount of magnetic counterpart, namely, barium hexaferrite for applications in S, C, and X-bands. Effective dielectric permittivity and magnetic permeability were measured using cavity perturbation method in the frequency range of 2–12 GHz. The microwave absorbing characteristics of the composites were studied in the S, C, and X-bands employing a model in which an electromagnetic wave is incident normally on a metal terminated single layer. Reflection loss exceeding −20 dB is obtained for all the samples in a wide frequency range of 2–12 GHz when an appropriate absorber thickness between 5 and 9 mm is chosen. The impact of carbon black is clearly observed in the optimized composites on the mechanical strength, thickness, band width of absorption, dielectric properties, and absorptivity. © *2014 AIP Publishing LLC*. [http://dx.doi.org/10.1063/1.4886382]

I. INTRODUCTION

Flexible microwave absorbers with required mechanical properties are increasingly in demand and necessary due to stricter environmental protection rules enacted by the federal agencies. The fourth and rising source of environmental pollution, electromagnetic interference (EMI), caused by mobile communication devices (0.8–1.5 GHz), local area networks (2.45, 5, 1, 22, and 60 GHz), and radar (11.7–12.0 GHz) are potential hazards to biological systems.[1] The avalanche growth of electronic devices in telecommunication systems operating in the S and X-bands is another source of electromagnetic pollution.[2–5] Hence, efficient electromagnetic wave absorbers with superior qualities which cater to the above bands are sought after.

One significant advantage of choosing a composite material as absorber is that by a judicious choice of filler particles in the elastomeric matrix, magnetic, and dielectric properties along with hardness, mouldability, and flexibility can all be tailored in a single material.[6–9] Dielectric loss and magnetic loss are the two main prerequisites in the design of a microwave absorber. Lossy dielectrics like Natural rubber, Butyl Rubber, and Nitrile rubber are an immediate choice for matrix since they can be moulded into definite shapes or can be made into flexible sheets. Nitrile-butadiene rubber (NBR) stands out among other elastomers since it offers excellent resistance to oils and acids than natural rubber. With increasing the amount of ACN (acrylonitrile) content, the molecules become more polar accompanied by an enhancement in dielectric permittivity. Carbon black (CB) is an ideal dielectric companion due to its low cost and easy processability compared to other carbon allotropes. Moreover, CB reinforces the rubber matrix by improving the tensile strength without disturbing the elastic properties of rubber.[9] It is thus imperative that a lossy dielectric like rubber can serve as the matrix and for imparting the required magnetic characteristics, different magnetic fillers can be incorporated. Among ferrites, hexagonal ferrites satisfy the requirements of a lossy magnetic material in the GHz frequency range in accordance with high Snoek's limit.[10] Moreover, hexagonal ferrites have high magnetic permeability, magnetization, and tunable anisotropic field.[11–13]

Microwaves, when incident on a lossy dispersive material, create heating within the material through various phenomena/mechanisms. This dissipation is mainly due to two material parameters: the complex dielectric permittivity and the complex magnetic permeability. The real parts are associated with energy storage and the imaginary parts are related to the loss or energy dissipation within the material resulting from conduction, resonance, spin inversions, and relaxation processes.[2,3] If the surface impedance of the absorbing material closely matches with that of the air, the reflections from the surface, which are backed by a perfect reflector (metal), are minimized. This condition favors the incident wave propagation into the material, where the energy is dissipated and/or absorbed, demonstrating the loss factor increase in the material. In the present study, we have employed surface

a)Author to whom correspondence should be addressed. Electronic mail: mraiyer@yahoo.com. Fax: +91 484 2577595.

impedance modeling based on transmission line theory for calculating the reflection loss (RL) and impedances by assuming that electromagnetic waves are incident normally on a single layer absorber backed by a perfect conductor. The effective complex dielectric permittivity and magnetic permeability evaluated using cavity perturbation technique served as an input to the surface impedance modeling.

Literature is replete with extensive studies on composites containing various fillers and their suitability as microwave absorbers. For example, Brosseau *et al*. carried out systematic investigations on composite materials by impregnating CB and other carbonaceous material in various matrices.[14–22] They also evaluated the microwave absorbing properties of composite materials by incorporating magnetic fillers in non magnetic matrices.[23–25] We carried out extensive investigation on composites containing magnetic and nonmagnetic fillers in various rubber matrices[26–32] and very recently on rubber-hexaferrite-carbon black (CB) composite with strontium hexaferrite (SrF) as the magnetic component.[33] Barium hexaferrite (BaF) also belongs to the hexagonal family of ferrites and in the present investigation SrF is replaced with BaF. This investigation primarily focuses on enhancing the absorption bandwidth and impedance matching by incorporating an optimum amount of magnetic component along with CB. The minimum thickness for maximum absorption will be estimated using the surface impedance model. The impact of BaF on the bandwidth of absorption will also be dealt with. A composition corresponding to a loading 80 phr (part per hundred rubber by weight) of BaF was chosen as the optimum amount of filler for further loading of CB, and the weight percentage of CB was varied in parts per hundred of rubber from 10 to 50 in steps of 10.

II. EXPERIMENTAL

Four composite samples were prepared by compounding nitrile rubber, 80 phr BaF, and different loadings of CB (HAF N-330) from 30 phr to 50 phr with an increment of 10 according to a specific recipe. The rubber-hexaferrite-CB composites were prepared using the synthesised BaF powder and raw gum rubber sample. For this BaF was synthesized using ceramic techniques here in the laboratory. Initial blending of various ingredients with gum rubber was carried out in a Brabender Plasticoder. The compound material is removed from the mixing chamber and further homogenized in a two-roll mill operated with a friction ratio of 1:1.25. The compound was passed endwise six times through the two-roll mill, with a tight nip and finally rolled into a sheet by keeping the nip at a separation of 3 mm. The composite sheets were aged for 24 h before being readied for further characterization. The samples were coded for ease of identification, and the prepared samples are listed in Table I with description. Dumb-bell shaped sample pieces are cut using a die with a cross section of 2 mm × 2 mm from these sheets for the evaluation of the mechanical properties as well as for the measurement of effective complex dielectric permittivity and magnetic permeability. Effective complex dielectric permittivity and magnetic permeability were measured by employing cavity perturbation technique using a cavity

TABLE I. Sample codes and their description.

Sample codes	Description
80BaF	80 phr BaF in NBR
30CBBaF	30 phr CB and 80 phr BaF in NBR
40CBBaF	40 phr CB and 80 phr BaF in NBR
50CBBaF	50 phr CB and 80 phr BaF in NBR
Blank	100 phr NBR

resonator and a two port Vector Network Analyzer (VNA). For S-band (2–4 GHz), cavity is connected to a two port vector network analyzer (ZVB4, Rohde & Schwaz) and for X-band (8–12 GHz) measurements the cavity is connected to a four port Agilent network analyzer through coaxial cables. Cavity is a rectangular waveguide with dimensions properly chosen to have resonance of electromagnetic waves for a predetermined TE_{10n} mode to sustain in the cavity of frequency range of interest and connected to a vector network analyzer through coaxial cables. In the cavity perturbation technique, the sample is inserted in the maximum field positions to perturb the fields through the slot as shown in Figure 1(a), so as to measure the permittivity and permeability.[34,35] Figures 1(b) and 1(c) depict the magnetic and electric field line patterns, respectively, in the standing wave of a typical TE_{101} mode. The reflection loss of composites backed by a perfect reflector can be derived from the measured complex dielectric permittivity and magnetic permeability using transmission line theory.[14,36]

A single layer absorber backed by perfect reflector in air works on the principle of impedance matching between air ($Z_0 = \sqrt{\frac{\mu_0}{\varepsilon_0}}$) and absorber material ($Z_{in} = \sqrt{\frac{\mu\mu_0}{\epsilon\epsilon_0}}$), where μ_0 and ε_0 are, respectively, the permeability and permittivity of vacuum, while μ and ε are the relative magnetic permeability and relative dielectric permittivity of the material. A perfect impedance match $Z_{in} = Z_0$ permits electromagnetic waves to propagate from free space to the inside of the absorber without any reflection. For the condition $Z_{in} = Z_0$, μ and ε are essential to be equal. The total absorption mostly arises from the effective magnetic loss and dielectric loss as discussed in the introduction. Absorption also depends on the thickness of the absorber. Minimum sample thickness for maximum absorption is dependent upon the permeability and permittivity of the material. For a metal-backed absorber, the reflection loss R can be expressed as

$$R = 20\,\mathrm{Log}_{10}|\Gamma|\mathrm{dB}, \tag{1}$$

where R is the reflection loss in decibels (dB) and Γ is the reflection coefficient

$$\Gamma = \frac{Z_{in} - 1}{Z_{in} + 1}. \tag{2}$$

For a single layer absorber, the input impedance Z at the front surface of the reflector backed material layer is given by

$$Z_{in} = Z_0\sqrt{\frac{\mu}{\varepsilon}}\tanh\left[j\left(\frac{2\pi ft}{c}\right)\sqrt{\mu\varepsilon}\right], \tag{3}$$

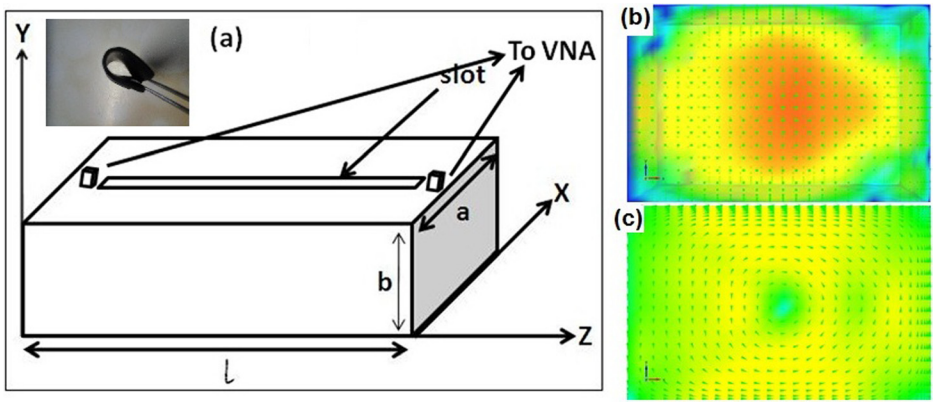

FIG. 1. (a) Schematic diagram of a rectangular cavity resonator. Inset displays the flexibility of sheets. (b) Electric field line and (c) magnetic field line distributions of TE_{101} mode standing wave (top view).

where c is the velocity of light; t is the thickness of the material; f is the frequency of the incident wave; $\mu = \mu' - j\mu''$ is the effective complex magnetic permeability; and $\varepsilon = \varepsilon' - j\varepsilon''$ is the effective complex dielectric permittivity.

X-ray diffraction (XRD) patterns of the samples were recorded using Rigaku D Max and the structural parameters were evaluated. The fractured surface morphology of representative composite samples was examined using a Scanning Electron Microscope (SEM, JSM-6390LA). Parameters, namely, tensile strength, modulus at different strain and elongation at break, which are some of the indicators of mechanical properties, were evaluated using a universal testing machine (UTM), model Instron 4500. Hardness was measured using a Durometer type A.

III. RESULTS AND DISCUSSION

XRD patterns of the composites were recorded on a Rigaku X-ray diffractometer with Cu K_α source are shown in Figure 2. The characteristic peaks of BaF are clearly visible in all the samples. A broad peak centered approximately at 19° is observed for blank rubber sample and which is due to short range orientation of polymer molecules of cured rubber. Diffraction peaks marked Z correspond to ZnO, an ingredient in the recipe. The broad peak at 19° vanishes with increasing BaF content and peaks corresponding to BaF start to appear in the diffraction pattern. There are no apparent shifts in the positions of the diffraction peaks of BaF and this

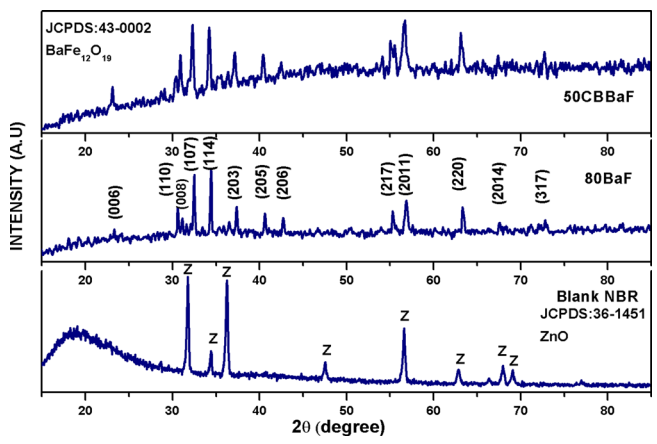

FIG. 2. XRD pattern of NBR-BaF-CB composites. 80BaF represents 80 phr BaF in NBR and 50CBBaF represents 50 phr CB and 80 phr BaF in NBR.

indicates that BaF has not undergone any structural change due to the heat treatment process during curing.

Morphological studies by SEM of the fractured surfaces of representative composite samples are cited in Figure 3. Figures 3(a) and 3(c) are samples corresponding to 80BaF, while Figs. 3(b) and 3(d) represent 50CBBaF. Agglomerates and rods shaped particles are also visible in the micrographs, which are confirmed to be BaF by Electron Dispersive Spectroscopy.

Room temperature magnetic hysteresis loops for the composite sample 80BaF and pure BaF are shown in Figure 4. It can be noticed that these samples do not get saturated even at a higher applied fields like 15 kOe. This is associated with random orientation of crystallographic c-axis, which is the direction of easy magnetization of hexaferrite particles. There is no apparent change in coercivity with respect to pure BaF, while saturation magnetization of the composite diminished considerably and as expected due to the presence of non magnetic constituents like CB and NBR.

The effect of CB on the tensile properties of composites is shown in Table II. The incorporation of ferrite filler reinforces the NBR matrix and showed a maximum reinforcement in the presence of CB. The modulus increased only nominally with the addition of ferrite filler, whereas the increase was appreciable with addition of CB. The elongation at break decreased and hardness increased with the addition of both fillers.

Frequency dependent effective complex dielectric permittivity and magnetic permeability of the composite samples measured in the range of 2–4 GHz and 8–12 GHz are depicted in Figure 5. ε' increases monotonically with increasing CB content due to increase in interfacial polarisation. Composite containing 80BaF registered a value of 4 for ε', while ε' recorded a value of 14 after impregnation of 50 phr CB. The variation of effective complex dielectric permittivity with frequency was further modelled by Maxwell Garnett's and Bruggemann's effective medium theories and found to be in agreement with the experimental results.[37] The corresponding imaginary part also exhibited an enhancement and displayed dispersions. The imaginary part of effective complex dielectric permittivity (ε'') showed a relaxation peak at around 10.5 GHz. Corresponding to this peak a decrease in permittivity is also visible as evident from Figure 5(a). In a complex hexagonal structure of M-type BaF, positive and negative ions of different valences are

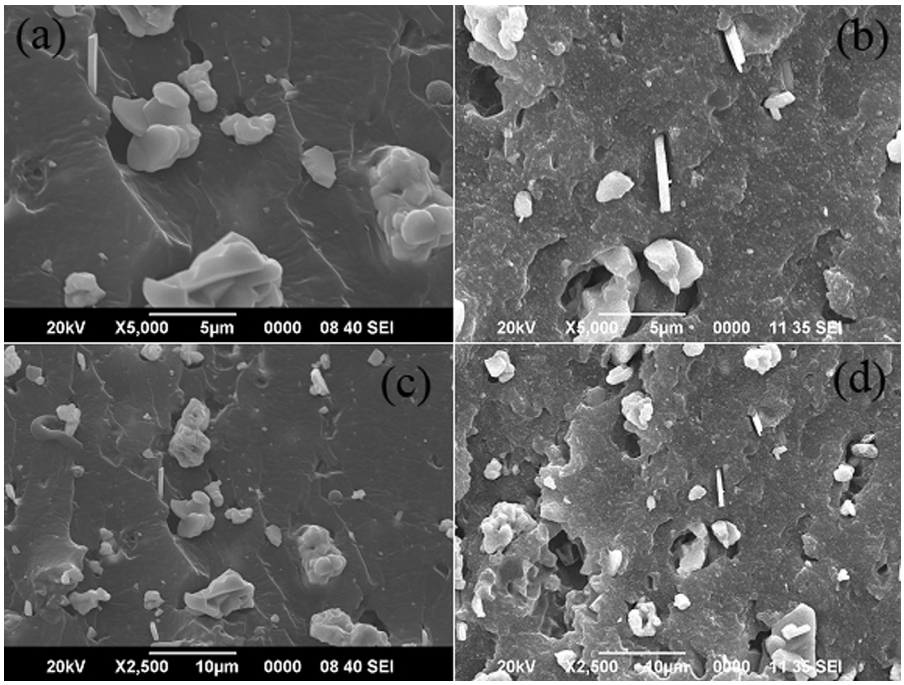

FIG. 3. Scanning electron micrographs of fractured surface of samples (a) and (c) for 80BaF and (b) and (d) for 50CBBaF at two different resolutions.

separated at varying bond lengths, generating dipole moments of varying strengths, giving rise to dipolar polarization. The heterogeneous structure of Rubber Ferrite Composites (RFC) comprising conducting ferrite grains separated by non-conducting polymer as well as CB reinforced polymer layers give rise to interfacial polarization. The matrix material NBR also contributes to the total polarisation due to polar groups attached in its polymer chain. The dielectric loss corresponds to the phase lag of the dipole oscillations with respect to the external field. The conduction in ferrites is attributed to the existence of both ferrous and ferric ions and electron hopping mechanisms.[38] Moreover, when the frequency of electron hopping between Fe^{3+} to Fe^{2+} ions matches that of microwave frequency, dielectric resonance occurs, which is responsible for the relaxation peak centred at 9.8 GHz as shown in Figure 5(b). There is a minimal increment in the value of dielectric loss at around 3.6 GHz while there is no corresponding decrease in the real part of effective permittivity. Hence, the exact loss mechanism is rather unclear.

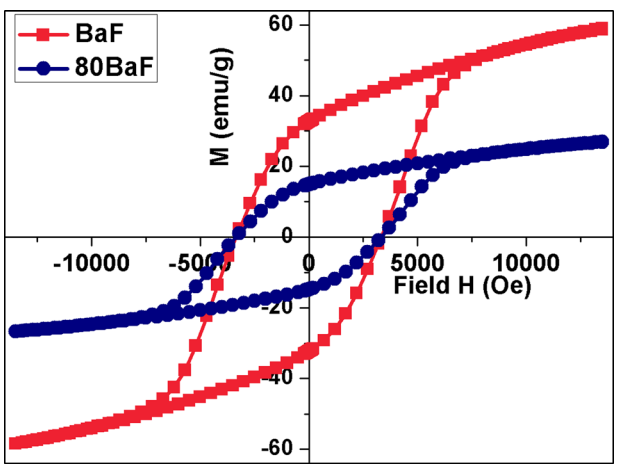

FIG. 4. Hysteresis loops for 80BaF and pristine BaF powder.

Since the magnetic characteristics of the composite samples depend only on the hexaferrite filler (BaF) and hence the variation of effective magnetic permeability with frequency almost remains the same for all the four samples (Figures 5(c) and 5(d)). It can be observed that the real part of effective magnetic permeability decreases with increase in frequency. The imaginary part of permeability, μ'', exhibits a peak at 7.67 GHz. 80BaF with an anisotropic field $H_a = 2.79$ kOe displays a ferromagnetic resonance $f_r = \gamma H_a$ at 7.8 GHz, where $\gamma = 2.8$ MHz/Oe is the gyromagnetic ratio.[38] The observed μ'' as shown in Figure 5(d) is in good agreement with the kind of mechanism of natural magnetic resonance. The ferromagnetic resonance frequency is expected to decrease considerably with increase in volume fraction of BaF filler as H_a is inversely proportional to saturation magnetization. The lower values of permeability and weak dispersion seen in these samples are attributed to the presence of non-magnetic constituents like CB and NBR between the neighboring crystallites, which weakens the magnetic interactions.

Figure 6 shows the frequency dependence of the calculated reflection loss of the NBR-BaF-CB composites in the frequency range of 4–12 GHz for different thicknesses. The matching thickness of the reflection loss minima decreases with increase of CB content. It is noteworthy that the intensity and frequency of the reflection loss are minimal for composites. Composites containing CB showed superior microwave

TABLE II. Effect of CB on the mechanical properties of composites.

Filler loading	Tensile strength (MPa)	Young's modulus (MPa)	Elongation at break (%)	Hardness
Blank NBR	2	2.15	469	55
80BaF	3.19	2.16	440	65
30CBBaF	15.26	9.6	410.1	76
40CBBaF	19.02	11.68	389.7	78
50CBBaF	20.76	15.39	345.3	81

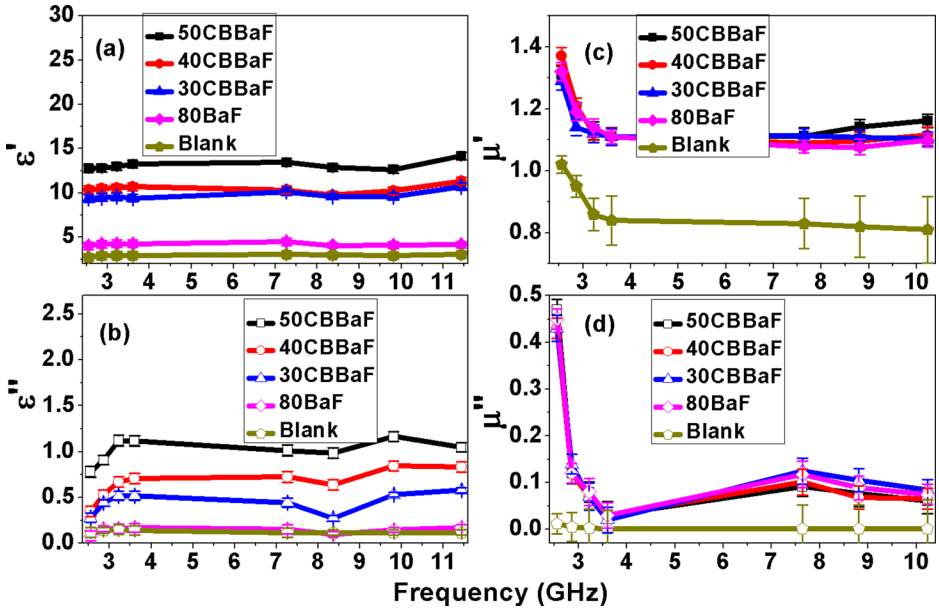

FIG. 5. Frequency dependence of effective complex dielectric permittivity and magnetic permeability in the range of 2–12 GHz.

absorption in the frequency range of 6–12 GHz (X-band) with −47 dB reflection loss at 11 GHz with a matching thickness of 6 mm for 30CBBaF. All samples display a reflection loss greater than −20 dB which is the standard value for a typical electromagnetic absorber with 99% absorption, except 80BaF. In the frequency range of 2–4 GHz (Figure 7), composites exhibit a maximum reflection loss of −27 dB at 2.5 GHz for 50CBBaF for a thickness of 7 mm. At 2–12 GHz, the minimum reflection shifts towards lower frequency with an increase in matching thickness for each sample. The thickness for complete cancellation of reflection lies in between 5 mm to 9 mm for different CB added composites.

In Table III, the microwave absorption properties of all the samples are listed and a comparison is made. The absorber thickness denotes the thickness range for complete cancellation of the incident and reflected wave in which RL ≤ −20 dB. Maximum RL value represents the largest absolute value of reflection loss. The absorption band width signifies the frequency range for which RL ≤ −10 dB. It can be observed that the composite containing 30CBBaF displays superior absorption and possess broader absorption bandwidth at a lower volume fraction of CB for a thinner absorber in the C and X-bands. The enhancement is due to excellent impedance matching between the magnetic BaF and the dielectric, CB and NBR.

These results are in fairly good agreement with our earlier published work.[33] The effective permeability and permittivity measured in the X-band for pure barium ferrite are in good agreement with that of measured in this investigation.[39] There are numerous reports in the context of CB and polymer composite with very good absorbing properties.[14–22,40–43] Here, the enhancement of impedance matching, absorption bandwidth,

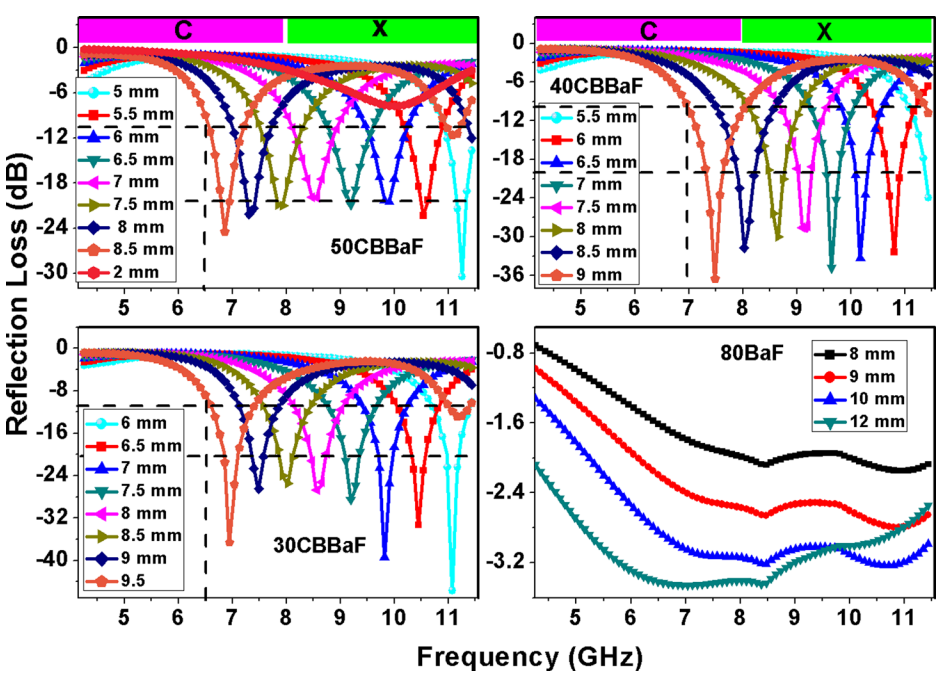

FIG. 6. Reflection loss for different thicknesses in the C and X-bands.

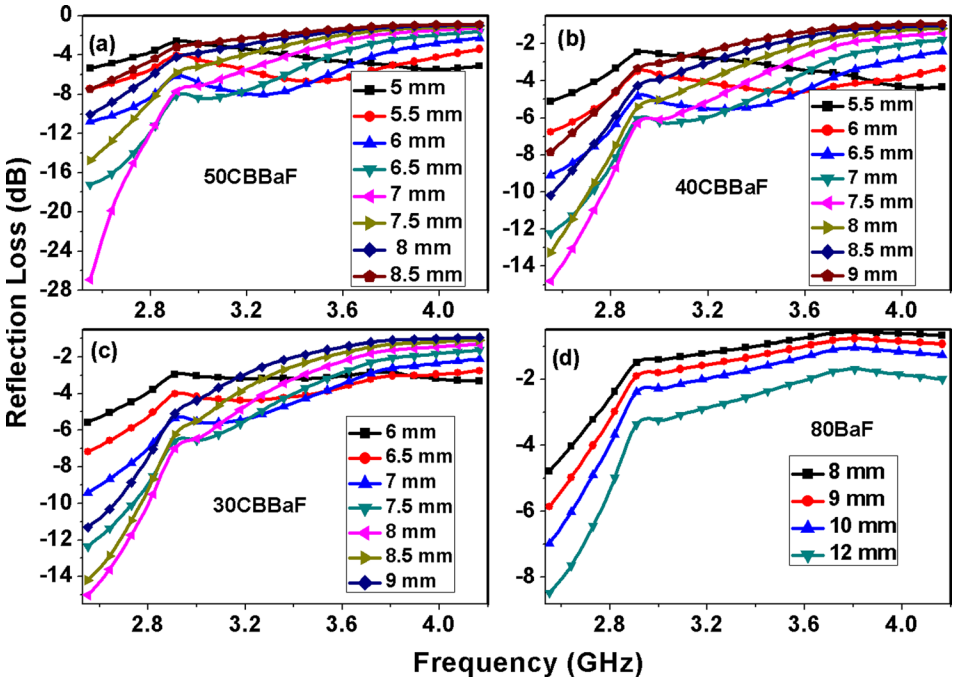

FIG. 7. Reflection loss for different thicknesses in the S-band.

and mechanical properties by incorporating an optimum amount of barium hexaferrite along with CB is examined.

IV. CONCLUSIONS

Thin, light, flexible, and easy to install absorber sheets have been fabricated by incorporating BaF and CB in an elastomeric matrix of NBR. The composites consisting of BaF and CB in nitrile rubber matrix exhibited good electromagnetic absorbing ability in the frequency range of 2–12 GHz. Embedding carbon black not only enhances electromagnetic absorption but also reinforces the rubber matrix with improved tensile strength without affecting the elastic properties of rubber. Among the four samples tested for absorption, composite containing 30CBBaF possess minimum reflection loss reaching −47 dB at a frequency of 11 GHz for a thickness of 6 mm. Reflection loss values exceeding −20 dB (99%) in any frequency interval of C and X-bands can be obtained by choosing an appropriate absorber thickness between 5 and 9 mm. By tuning the content of CB, the absorption capability was successfully altered, and as a result, the composites achieved significant microwave absorption.

TABLE III. Microwave absorption bandwidth and minimum thickness for the composite samples.

Material	CB volume fraction	Absorber thickness (mm)	Maximum RL value (dB)	Absorption band width (GHz)
50CBBaF	0.051	5–8.5	−27	2.5–2.8
			−31	6.5–11.5
40CBBaF	0.042	5.5–9	−15	2.5–2.85
			−37	7–11.5
30CBBaF	0.034	6–9.5	−15	2.5–2.9
			−46	6.5–11.5
80BaF	0	8–12	−9	…
			−3.5	
NBR-blank	0	13–17	−1.3	…

V. SUPPORTING DATA

A. Crystallinity of the polymer matrix

The crystallinity of Nitrile Butadiene Rubber decreases with increase of carbon black CB. This information is drawn based on the X-ray diffraction data. The amorphous peak centered at 19.5 corresponds to NBR phase. The addition of fillers destroys the crystallinity of the composite and crystallinity almost vanishes as depicted in Figure 8.

B. Magnetic loss and dielectric loss of constituents

The effective magnetic loss and dielectric loss of the constituents of the composite are shown in Figures 9 and 10, respectively. It is to be noted that the resonance peak presented in the imaginary part of effective permeability for the barium hexaferrite is absent in the case of pure hexaferrite (Figure 9). This is due to the shift in resonance peak to

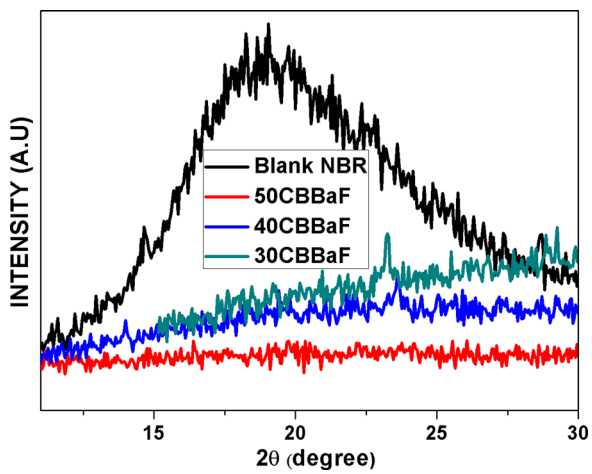

FIG. 8. Enlarged view of XRD of different composite samples at 2 theta values from 10 to 30.

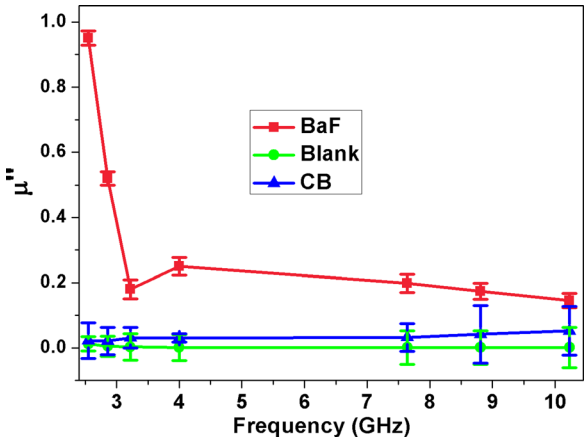

FIG. 9. Variation of magnetic loss with frequency of pristine samples.

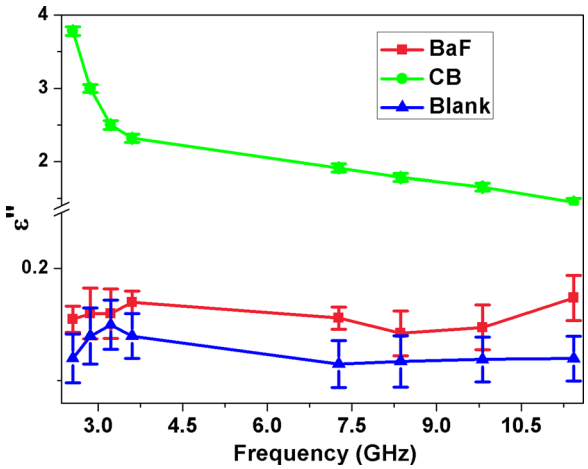

FIG. 10. Variation of dielectric loss with frequency of pristine samples.

lower frequency (C-band) as saturation magnetization is inversely proportional to the crystalline anisotropy filed H_a. $H_a = 2\,K/M_s$, where K is called anisotropy constant. Since we have done interpolation through C-band by measuring S and X-bands, the behavior in C-band is unknown. Rectangular shaped samples of dimension $3 \times 3 \times 40$ mm have been prepared by applying pressure to fine powders of CB and BaF for employing cavity perturbation technique.

ACKNOWLEDGMENTS

This work was supported by All India Council for Technical Education (File No. 8023/RID-73/2004-05 dated 29/03/2005), Government of India. S.V. acknowledges University Grants Commission (Order No.F.14-2(sc)/2009(SA-III) dated 18/12/2010) for financial assistance in the form of a fellowship. We thank Dr. K. C. James Raju, School of Physics, University of Hyderabad, India, for providing the electromagnetic field distribution of TE_{101} mode image simulated using COMSOL Multiphysics®.

[1]X. F. Zhang, H. Huang, and X. L. Dong, J. Phys. Chem. C **117**, 8563 (2013).
[2]A. N. Yusoff, M. H. Abdullah, S. H. Ahmad, S. F. Jusoh, A. A. Mansor, and S. A. A. Hamid, J. Appl. Phys. **92**, 876 (2002).
[3]J. R. Liu, M. Itoh, T. Horikawa, K.-i. Machida, S. Sugimoto, and T. Maeda, J. Appl. Phys. **98**, 054305 (2005).
[4]Y. He, R. Gong, Y. Nie, H. He, and Z. Zhao, J. Appl. Phys. **98**, 084903 (2005).
[5]R. Lv, F. Kang, J. Gu, X. Gui, J. Wei, K. Wang, and D. Wu, Appl. Phys. Lett. **93**, 223105 (2008).
[6]K. A. Malini, E. M. Mohammed, S. Sindhu, P. A. Joy, S. K. Date, S. D. Kulkarni, P. Kurian, and M. R. Anantharaman, J. Mater. Sci. **36**, 5551 (2001).
[7]K. A. Malini, P. Kurian, and M. R. Anantharaman, Mater. Lett. **57**, 3381 (2003).
[8]M. A. Soloman, P. Kurian, M. R. Anantharaman, and P. A. Joy, J. Elastomers Plast. **37**, 109 (2005).
[9]M. A. Soloman, P. Kurian, M. R. Ananthraman, and P A. Joy, Indian J. Chem. Technol. **12**, 582 (2005).
[10]J. L. Snoek, Physica **XIV**, 4 (1948).
[11]M. Matsumoto and Y. Miyata, J. Appl. Phys. **79**, 5486 (1996).
[12]P. Xu, H. Xijiang, and W. Maoju, J. Phys. Chem. C **111**, 5866 (2007).
[13]G. Mu, C. Na, P. Xifeng, S. Haigen, and M. Gu, Mater. Lett. **62**, 840 (2008).
[14]F. Qin and C. Brosseau, J. Appl. Phys. **111**, 061301 (2012).
[15]C. Brosseau, F. Boulic, P. Queffelec, C. Bourbigot, Y. Le Mest, J. Loaec, and A. Beroual, J. Appl. Phys. **81**, 882 (1997).
[16]A. Mdarhri, F. Carmona, C. Brosseau, and P. Delhaes, J. Appl. Phys. **103**, 054303 (2008).
[17]A. Mdarhri, C. Brosseau, and F. Carmona, J. Appl. Phys. **101**, 084111 (2007).
[18]C. Brosseau, P. Molinié, F. Boulic, and F. Carmona, J. Appl. Phys. **89**, 8297 (2001).
[19]C. Brosseau, A. Mdarhri, and A. Vidal, J. Appl. Phys. **104**, 074105 (2008).
[20]C. Brosseau, W. NDong, and A. Mdarhri, J. Appl. Phys. **104**, 074907 (2008).
[21]B. J.-P. Adohi, A. Mdarhri, C. Prunier, B. Haidar, and C. Brosseau, J. Appl. Phys. **108**, 074108 (2010).
[22]C. Brosseau and M. E. Achour, J. Appl. Phys. **105**, 124102 (2009).
[23]C. Brosseau and P. Talbot, J. Appl. Phys. **97**, 104325 (2005).
[24]C. Brosseau, S. Mallégol, P. Quéffelec, and J. B. Youssef, Phys. Rev. B **70**, 092401 (2004).
[25]V. Castel, C. Brosseau, and J. Ben Youssef, J. Appl. Phys. **106**, 064312 (2009).
[26]T. N. Narayanan, V. Sunny, M. M. Shaijumon, P. M. Ajayan, and M. R. Anantharaman, Electrochem. Solid-State Lett. **12**(4), K21 (2009).
[27]M. A. Jamal, P. Mohanan, P. A. Joy, P. Kurian, and M. R. Anantharaman, Appl. Phys. A **97**(1), 157–165 (2009).
[28]M. A. Jamal, P. Kurian, P. A. Joy, and M. R. Anantharaman, Mater. Chem. Phys. **121**, 154 (2010).
[29]V. Sunny, P. Kurian, P. Mohanan, P. A. Joy, and M. R. Anantharaman, J. Alloys Compd. **489**, 297 (2010).
[30]V. Sunny, W. Tabis, D. S. Kumar, Y. Yoshida, P. Mohanan, and M. R. Anantharaman, Mater. Lett. **64**, 1130 (2010).
[31]E. Muhammad Abdul Jamal, P. A. Joy, P. Kurian, and M. R. Anantharaman, Polym. Bull. **64**, 907 (2010).
[32]R. Kumar Srivastava, T. N. Narayanan, A. P. Reena Mary, M. R. Anantharaman, A. Srivastava, R. Vajtai, and P. M. Ajayan, Appl. Phys. Lett. **99**, 113116 (2011).
[33]S. Vinayasree, M. A. Soloman, V. Sunny, P. Mohanan, P. Kurian, and M. R. Anantharaman, Compos. Sci. Technol. **82**, 69 (2013).
[34]B. Viswanathan and V. R. K. Murthy, *Ferrite Materials: Science and Technology* (Narosa, New Delhi, 1990), p. 72.
[35]A. Parkash, J. K. Vaid, and A. Mansingh, IEEE Trans. Microwave Theory. Tech **27**, 791 (1979).
[36]K. J. Vinoy and R. M. Jha, *Radar Absorbing Materials—From Theory to Design and Characterization* (Kluwer Academic Publishers, Boston, MA, 1996).
[37]C. Brosseau, J. Phys. D: Appl. Phys. **39**, 1277 (2006).
[38]P. Singh, V. K. Babbar, A. Razdan, R. K. Puri, and T. C. Goel, J. Appl. Phys. **87**, 4362 (2000).
[39]A. Bahadoor, Y. Wang, and M. N. Afsar, J. Appl. Phys. **97**, 10F105 (2005).
[40]L. Liu, Y. Duan, L. Ma, S. Liu, and Z. Yu, Appl. Surf. Sci. **257**, 842 (2010).
[41]J.-H. Oh, K.-S. Oh, C.-G. Kim, and C.-S. Hong, Composites, Part B **35**, 49 (2004).
[42]P. Annadurai, A. K. Mallick, and D. K. Tripathy, J. Appl. Polym. Sci. **83**, 145 (2002).
[43]W. Meng, D. Yuping, L. Shunhua, L. Xiaogang, and J. Zhijiang, J. Magn. Magn. Mater. **321**, 3442 (2009).